

ORIGINAL RESEARCH PAPER

Experimental Investigation of the Effect of Circular Cutout Trigger on Energy Absorption of Three-layered Steel/Polypropylene/Aluminum Deep Drawn Cups

A. Nassiri, A. Atrian*

Department of Mechanical Engineering, Najafabad Branch, Islamic Azad University, Najafabad, Iran.

Article info

Article history:

Received 02 October 2020

Received in revised form

03 December 2020

Accepted 03 December 2020

Keywords:

Deep drawing

Sandwich panel

Composite

Energy absorption

Geometrical trigger

Abstract

In this paper, energy absorbing characteristics of aluminum/polypropylene/steel sandwich cups are investigated. To this end, sandwich panels were fabricated using hot pressing technique. Then the panels were deep drawn using a circular punch to produce three-layer cups. Subsequently, the cups were axially compressed (crushed) under quasi-static deformation in order to investigate their energy absorption capacity. Finally, the effects of thickness of polypropylene layer as well as circular cutout triggers on energy absorption of the sandwiched cups were evaluated. The results show that changing the thickness of polypropylene layer from 1 to 2mm could successfully increase the energy absorption by about 24%. Furthermore, adding geometrical triggers like circular cutouts with radius of 2.5mm could reduce the absorbed energy from 346J in the sample without trigger to about 335J in the sample with trigger (3.2% reduction). The trigger could also reduce the peak force near 14% (from about 29kN to about 26kN) that can be considered as a positive point of triggers to mitigate damage in the samples.

1. Introduction

With increase in air pollution due to extensive use of fossil fuels in transportation vehicles (cars, trucks, ships and airplanes), the need for wisely designing of such vehicles in order to reduce fuel consumption has become more significant. On the other hand, the need for better safety and reliability of vehicles during accidents or unpredictable collisions motivates engineers to consider energy absorption as well as weight reduction as two key features during the design [1, 2]. In this regard, metal-polymer composite sandwich panels have gained special attention in energy absorption systems [3]. These panels often consist of a metal shell made of steel or aluminum alloys and a polymer core from

polypropylene or polyethylene [4]. Sandwich panels are often used as thin-walled or cylindrical structures under crushing loads for energy absorption purposes. Deep drawing is one of the processes used to create cylindrical structures [5, 6].

Crushing of cylindrical and thin-walled structures [7-10] is one of the methods of structural energy absorption [11, 12]. Regarding the rate of deformation, the absorbed energy can be measured through dynamic deformation (impact) or quasi-static deformation processes [13]. The energy absorbed by a cylindrical sample under quasi-static deformation can be easily calculated using force-displacement graph obtained by crushing process. In this order, some parameters such as maximum crushing force, crushing length, absorbed

*Corresponding author: A. Atrian (Associate Professor)

E-mail address: amiratrian@gmail.com

<http://dx.doi.org/10.22084/jrstan.2020.22215.1152>

ISSN: 2588-2597

energy, and Specific Absorbed Energy (SAE) may be introduced [2]. During quasi-static energy absorption, a sample is crushed at a constant speed. Although quasi-static tests might not be a precise representative of actual dynamic crushing processes, simplicity and easy control are the main reasons of utilizing quasi-static evaluations.

This study aims to investigate energy absorption of three-layered samples. Several other studies have investigated deep drawing process for fabrication of layered sheets [6, 14]. For example, Parsa et al. [15] used experimental and numerical studies to determine limiting draw ratio (LDR) of aluminum-polymer sandwich panels. Bagherzadeh et al. [16] also conducted analytical and experimental studies on hydro-mechanical deep drawing process for two-layered aluminum HO1050 and St13 steel sheets. Regarding measurement of energy absorption, Tsukamoto [17] investigated crushing behavior of deep drawn cups of two and six-layered aluminum/duralumin sheets and studied their use as energy absorbents and impact shields in vehicles. His results showed that six-layered samples have suitable behavior for use as impact absorbents. Furthermore, Alavi Nia et al. [5] studied the energy absorption capacity and collapse of cylindrical and rectangular thin-walled aluminum pipes under axial compression.

Jakirahemed et al. [7] showed that during energy absorption of expanded thin-walled pipes, the ratio of pipe expansion (outer diameter of the punch to inner diameter of the pipe) is the most important parameter for optimizing the peak force and increasing energy absorption capacity of samples. Some studies have also used geometrical triggers for optimizing the energy absorption and deformation time in energy absorbent structures [18, 19]. The reason for using geometrical triggers in energy absorbents is the stability of force during the crushing process. These triggers are simply applied at a specific area along the sample length and may lead the first folding (wrinkling) to occur at the trigger area under lower forces. The importance of this method is to prevent applying of larger forces to the entire structure that might damage the non-absorbent segments of the structure. This approach also creates a stable energy absorption during the crushing of cylindrical structures [18-20]. Han et al. [21] investigated the effects of holes created in aluminum and steel pipe structures during static and dynamic axial compression tests. They could also study the effects of these cutouts on energy absorption. Samer et al. [18] studied as well the effect of different oval, rectangular, and circular cutout triggers during static crushing test of rectangular thin-walled steel pipes. Hussain et al. [19] also compared the conditions and configurations of different trigger factors on the deformation pattern and crashworthiness of fiber-reinforced polymer composite samples.

The current study uses a novel form of sand-

wich panels using two different metals as two skins and a polymeric core. Polymeric core is believed to improve the mechanical damping properties of the sandwich structure [22]. To this end, aluminum/polypropylene/steel sandwich panels were fabricated using hot pressing process at 190°C and pressure of ~16MPa. Then the three-layered sandwich blanks were deep drawn to produce three-layered cups. Deep drawing process was already optimized in the authors' another paper [6] to find the most appropriate parameters including BHF, lubricant, and drawing depth. The cups were then subjected to axial compression in a quasi-static loading regime. Finally, the effect of middle layer thickness and presence of geometrical triggers, as a noticeable novelty in this research work, on energy absorption and deformation patterns of the samples were investigated, and some beneficial results were obtained.

2. Energy Absorption in Thin-walled Structures

In general, the main output of quasi-static crushing process, which is currently used to determine energy absorption, is a uniaxial force-displacement graph. This force-displacement graph may exhibit some important parameters as follows [23, 24] :

Maximum Crushing Force (P_{\max}):

This value indicates maximum force applied by jaws to the sample during the process. P_{\max} usually happens during the first step of loading when folding is just starting to occur. This parameter is essential in optimizing the design of energy absorbents and must be minimized. This force is the maximum force which can create permanent and stable deformation and wrinkling in the structure.

Total Absorbed Energy (E_{absorbed}):

This parameter shows the energy dissipated during structure deformation and is equal to the area under force-displacement graph:

$$E_{\text{absorbed}} = \int P d\delta \quad (1)$$

in which P and δ are the force and the crushing length, respectively.

Mean Crushing Force (P_m):

This parameter is the ratio of the measured absorbed energy to the total crushing length:

$$P_m = \frac{E}{\delta} \quad (2)$$

Specific Absorbed Energy (SAE):

This parameter is calculated as energy absorbed in a unit of mass (M) of each sample at effective crushing length:

$$SAE = \frac{E_{absorbed}}{M} \quad (3)$$

3. Materials and Methods

3.1. Fabrication of the Sandwich Panels

Using standard tensile test ASTM-E08 [25], stainless steel 304 and Al3105 sheets were selected as the skins, and thermoplastic polypropylene sheet (melting point of 180°C) was selected as the core. The tensile test was used to determine the behaviours and properties of metal sheets in order to select two alloys with compatible flow properties. Stainless steel and aluminum layers had 0.5mm thickness, while polymer layer was selected with two various thickness of 1 and 2mm. Table 1 shows the chemical analysis of aluminum and steel sheets obtained from Quantometric analysis.

In order to have a perfect deep drawing process, it is necessary to perform annealing process on the aluminum sheet in order to bring its tensile properties closer to that of steel sheet and in turn, to prevent it from tearing during deep drawing process. Therefore, aluminum sheets were annealed in a furnace for 30 minutes under temperature of 380°C and then cooled down to the room temperature [26]. Due to full annealing, aluminum sheets used in the current study are considered to have isotropic characteristics. Fig. 1 shows the stress-strain graphs of the used samples of steel, annealed aluminum, and polypropylene.

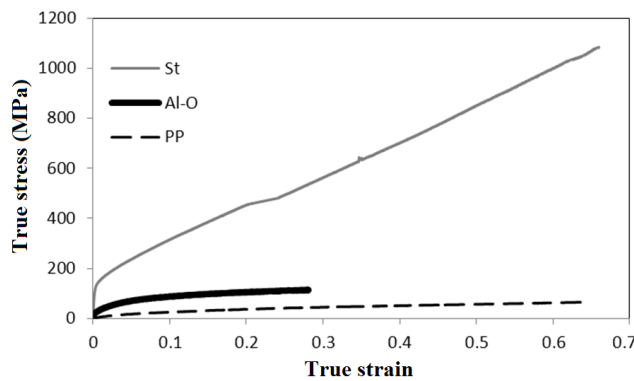


Fig. 1. True stress- strain graphs for polypropylene, steel, and annealed aluminum.

Table 1

Chemical properties of aluminum and steel sheets (obtained from Quantometer test).

Material	Constituents (%)								
Al3105	97.4 Al	0.76 Fe	0.57 Si	0.53 Mn	0.27 Mg	0.19 Cu	0.14 Zn	0.009 Cr	
St 304	70.7 Fe	18.5 Cr	8.39 Ni	1.27 Mn	0.48 Si	0.18 Co	0.1 V	0.06 C	

Three layers of aluminum, polymer, and steel were attached together using a granulated polymer adhesive with commercial name of Polypropylene Maleic Acid, which is one of the derivatives of polypropylene. To this end, it was necessary at first to remove metal oxide layers from the surfaces and then stick them together. The next step is creating a die for manufacturing sandwich panel sheets. This two-part die set was fabricated from ASTM A29 steel. The die first part is a billet with length of 300mm, width of 150mm, and thickness of 30mm on which two square holes with sides of 140mm are machined. The second part is a lid that is placed over the die (first part) after arranging all three layers inside it. In order to melt the granulated polypropylene adhesive between the sheets and adhere the sheets together, the mold is heated up to 190°C using a heating element mounted under the die [27]. A LASER thermometer was used to measure and control the temperature. After the temperature reached 190°C, the sample was kept under pressure of ~ 16MPa for 20 minutes and then held at the same pressure until the die was cooled down to near 50°C. As mentioned earlier, samples were prepared with polymer layer thickness of 1 and 2mm. The stacking sequence and schematic of manufacturing procedure are presented in Fig. 2.

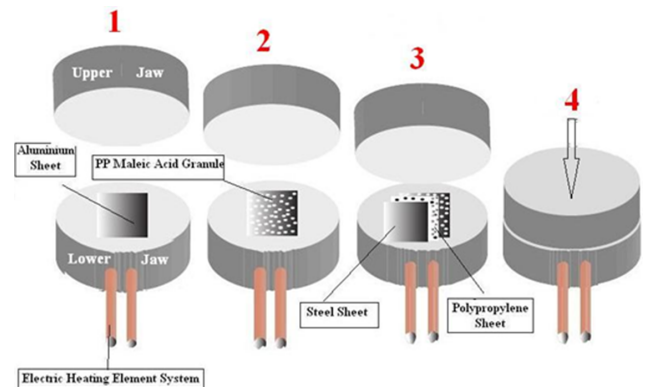


Fig. 2. Layer arrangement and fabrication process of Aluminum/Polypropylene/Steel sandwich panel. (1: Put the first metal layer, 2: Add the adhesive, 3: Complete the layers assembly, 4: Apply the pressure).

3.2. Deep Drawing Process

After preparing sandwich panels at two different thicknesses, they were cut into circular blanks with diameter of 130mm using waterjet process. Fig. 3 illustrates a cross-section of three-layered sandwich panel which shows aluminum, polypropylene and steel sheets from top to bottom, respectively.

The deep drawing die set (including blank holder and matrix) were also made from cast iron, while punch was made from ASTM A29 steel. Eight springs with stiffness of 161N/mm could control the BHF (Fig. 4). Table 2 shows the dimensions of the die set. It is noteworthy that due to having two different thicknesses, two punches with diameters of 63 and 65mm were used in the process. More details about the samples preparation and studying the deep drawing process parameters are presented in [6].

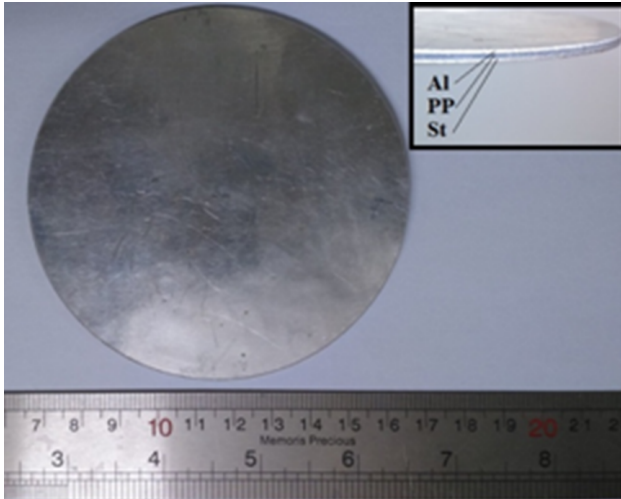


Fig. 3. Cross-section of three-layered aluminum/polypropylene/steel sandwich panels.

In order to investigate the effect of sheet thickness and BHF on behavior of the samples, six different BHF were adopted for sandwich panels with different thicknesses (more details will be presented in the next section). Nylon was used as lubricant in all the deep drawing processes to reduce the frictional forces and have a perfect process [6, 14].

Table 2
Dimensions of deep drawing die set.

Component	Outer diameter (mm)	Inner diameter (mm)	Profile radius (mm)
Punch	65	-	8
Matrix	230	69.4	10
Blank Holder	190	69	-

3.3. Geometrical Triggers

After deep drawing process, the edges of the samples were cut and circular cutouts were drilled as the geometrical triggers on the samples (Fig. 5). In the following sections, cup samples with 2 and 3mm thicknesses are denoted by S2 and S3, respectively. In this step, two sets of circular cutouts with different diameters and numbers were created on samples using drilling operation. It is assumed that the eliminated area from cup samples is constant in both set of cutouts. Therefore, based on simple calculations, two cutouts with radius of 3.5mm were created in the first set and 4 cutouts with radius of 2.5mm were created in the second set. Samples with two cutouts are shown as S2-2C-D7, and samples with 4 cutouts are shown as S2-4C-D5.

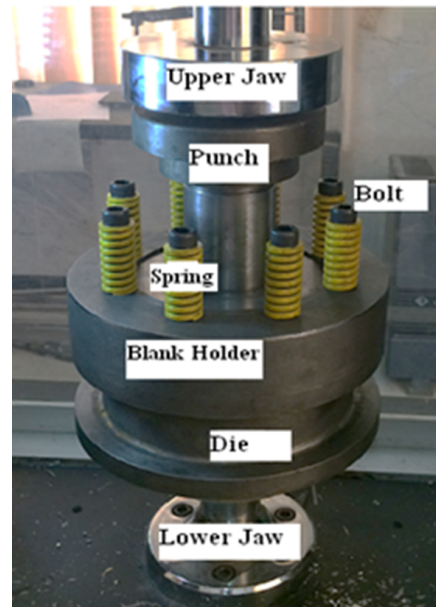


Fig. 4. Deep drawing die set.



Fig. 5. Sandwich deep drawn cups without edges; a) Without trigger, and b) With circular cutout triggers.

3.4. Crushing Tests

After inserting geometrical triggers on the deep drawn cups, all samples with or without trigger (intact sample) were tested separately under quasi-static axial crushing using SANTAM testing machine. The axial loading was applied with constant velocity of 10mm/min and could crush the samples up to 20mm. In these tests, the upper jaw of the machine moved down and pressed the closed end of the cups. In accordance with previous studies, no lubricants were used in energy absorption tests [15].

4. Results and Discussion

4.1. Studying the Deep Drawing Process

4.1.1. Effect of Layers Stacking Sequence

Based on the deformation properties of the layers, it was determined that layers should be arranged so that aluminum layer is in touch with the punch. Fig. 6 shows that if the layers are arranged in a way that steel layer is in touch with the punch, aluminum layer suffers from a premature tearing in the area of the punch profile diameter. This is because when aluminum layer is placed at the bottom, it has to tolerate higher strains. Similar results were also reported by Takuda et al. [28]. These researchers found that the draw-ability as well as the stretch formability in steel/aluminum laminated composite are improved by setting the mild steel sheet on the punch side.

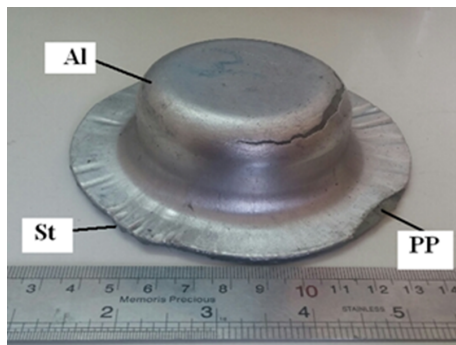


Fig. 6. Tears occurred at the deep drawn cup in the second layer arrangement (steel sheet touching the punch).

4.1.2. Effect of BHF

One of the most important parameters affecting the wrinkling of sheet edges during deep drawing process is the force applied by the blank holder. Fig. 7 shows the decreasing trend of wrinkling as the BHF increases. Table 3 shows the effects of BHF on the wrinkling height measured using a caliper. These results indicate that BHF directly affects the wrinkling of the blank edges. As can be seen, wrinkling height goes from its maximum value at around 8kN to near zero at BHF of ~ 12 kN. Higher BHFs act as a constraint against elastic circumferential buckling (elastic wrinkling) of the sample flange and force it to flow plastically. Moreover, higher BHFs give rise to more frictional forces which in turn, hinder freely sliding the flange over the die or the blank-holder. These two factors together lead to lower wrinkling under higher BHFs [6, 14]. Rajabi and Kadkhodayan [26] also reported similar wrinkling behavior for deep drawing of fiber-metal laminates.

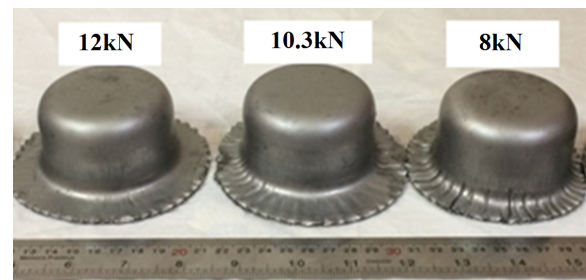


Fig. 7. Effects of BHF on wrinkling of samples flange.

4.2. Studying the Energy Absorption

4.2.1. Effect of Polymer Layer Thickness

The current research studies two groups of parameters and their effects on energy absorption of the composite deep drawn samples. In the first group, the effect of polymer layer thickness, and in the second group the effect of circular cutout triggers on energy absorption capabilities are investigated. Fig. 8 shows the deformation steps of S2 sample during a simple quasi-static crushing test. This sample lacks any geometrical triggers on its surface (intact sample) and shows symmetrical crushing at the beginning of the process due to the axial compression loading.

Table 3

Effects of BHF on wrinkling height (mm) for different thickness (t) and lubricants.

BHF (kN)	$t = 2\text{mm}$, Dry	$t = 2\text{mm}$, Nylon	$t = 3\text{mm}$, Dry	$t = 3\text{mm}$, Nylon
2.5	5.1	4.2	2.8	2.2
4.5	4.2	2.8	1.7	0.7
6.4	2.6	1.6	0.6	0
8	1.1	0.5	0	
10.3	0.4	0		
12	0			

From the start of the process, the sample shows signs of plastic deformation (Fig. 8, point A) and then exhibits initiation of axial plastic buckling (Fig. 8, point B). This deformation finally leads to full crushing of the sample (Fig. 8, point C). Generally in such experiments, when the material behavior transforms initially from elastic to plastic regime (Fig. 8b), and the first fold is appeared, a sudden drop in load-displacement curve may be observed (see point B in Fig. 9) [5].

Since the plastic and polymer compounds inherently damp the mechanical forces, it is expected to observe higher energy absorption in sample S3 which has a higher thickness of polymer layer, compared to sample S2. This expectation is clearly affirmed in Fig. 9 in which the area under load-displacement curve, or the absorbed energy, is higher for S3. Three points of A, B, and C in Fig. 8 are also marked on the corresponding load-displacement curve in Fig. 9 for better justification.



Fig. 8. Crushing process of sample S2 (thickness of 2mm): a) Start of crushing test, b) Start of buckling in the sample, and c) Sample after crushing.

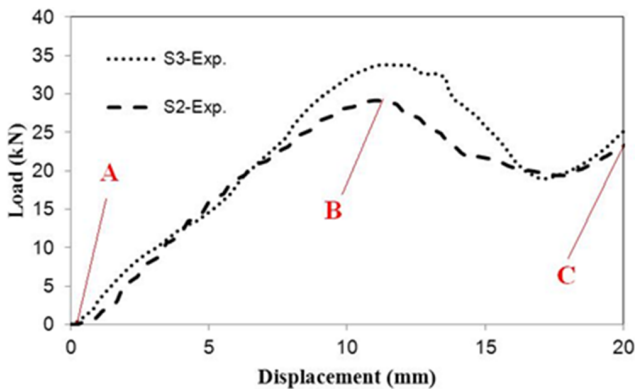


Fig. 9. Effect of middle layer thickness on force-displacement graphs.

Figs. 8 and 9 show that the crushing mode of intact samples of S2 and S3 before reaching to the maximum crushing force (region A to B) is relatively axisymmetric. After the maximum point (B) which corresponds to creation of the first plastic hinge, the load dropped smoothly. As the crushing process continues, the load ascended again to create the next fold (point C). Crushing mode associated to B-C region in Fig. 9 has also changed to asymmetric mode of progressive buckling (diamond) [9]. The absorbed energy and the specific adsorbed energy (ratio of the absorbed energy to the sample mass) are indicated in Fig. 10. Fig. 11 also expresses the maximum crushing force, the average crushing force, and the crushing distance at maximum force for both S2 and S3 samples.

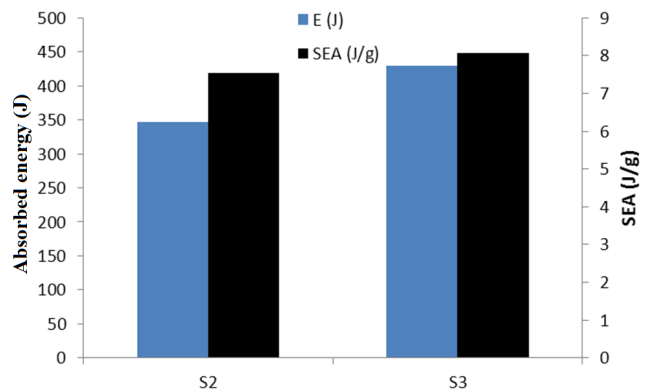


Fig. 10. The effect of polymer layer thickness on absorbed energy and specific absorbed energy (SAE).

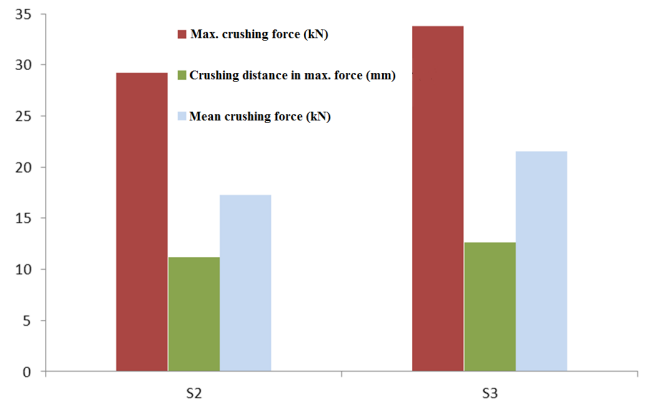


Fig. 11. The effect of polymer layer thickness on maximum crushing force, crushing distance at maximum force, and average crushing force.

As can be seen in these graphs, similar to the results reported by Praveen Kumar et al. [10], Cho et al. [29], and Kalhor and Case [30], increase in polymer layer thickness from 1 to 2mm creates more resistance against plastic deformation. This obviously leads to increase of the sample flow stress and in turn, to increase the maximum crushing force by about 16% (from 29.2kN in S2 to 33.8kN in S3). Increasing the thickness of polymer layer also causes delay in creation

of the first fold in the samples since the crushing distance in maximum force is higher for S3. This behavior may be attributed to the increased bending resistance of the laminated sheet with higher thickness. This result is also consistent with the findings of Goel [31]. It is also clear from Figs. 10 and 11 that by increasing the polymer layer thickness, the energy absorption improved by about 24%. The higher thickness of polymer layer also leads to the enhancement of the damping capability of the samples and make them more appropriate as the energy absorbing structures.

4.2.2. Effect of Geometrical Triggers

The aim of using geometrical triggers is to force the structure to enter the plastic deformation and nonlinear buckling phase a bit earlier than expected (compared to the structure without these triggers). This will result in faster yielding of the structure and therefore reduces the initial maximum crushing force applied to the structure. This ideally might increase the structure energy absorption since entering earlier to the first peak force generally leads to more steady behavior of the load-displacement curve and therefore to higher amounts of energy absorption [18, 32].

To get the expected efficiency of the triggers, they should insert to an appropriate location of the structure. The importance of applying triggers is to prevent intensive deformation and fracture through buckling of structure. This gives rise to a more stable and symmetrical wrinkling along the length of the specimen (based on the patterns of mechanical progressive buckling) while the crushing process starts at a lower first peak force [18]. Lower force for the first peak leads to lower chance of fracture in energy absorbent structures while ideally increases energy absorption capabilities [18].

Fig. 12 typically shows the crushing process of S2-2C-D7 cup sample at three steps of beginning of crushing (Fig. 12a), start of buckling in the sample (Fig. 12b), and at the end of crushing (Fig. 12c).

According to Fig. 13, it can be seen that the maximum crushing force for the samples with trigger (S2-4C-D5 and S2-2C-D7) was reduced by about 14% relative to the sample without any trigger (S2). Similar results were also reported by Abah et. al [33]. They showed as well that if circular openings add to tubular specimens, the mean load would maintain more steadily. In the current study, the cup sample with circular cutout triggers with diameter of 5mm has an energy absorption of 335.3 J (3.2% lower than that of S2 sample), while the sample with circular cutout triggers with diameter of 7mm has the energy absorption of 303 J (14.3% lower than that of S2 sample). Evidently, none of these triggers were useful in increasing energy absorption capacity of the three-layered cup samples. However, due to decrease in the first peak force, these

triggers can reduce the forces applied to the structure. Therefore, the triggers result in less damage in energy absorbent structure and other attached parts. On the other hand, geometrical triggers with diameter of 5mm have a better absorbing performance compared to triggers with diameter of 7mm since the former showed near 10% higher energy absorption.

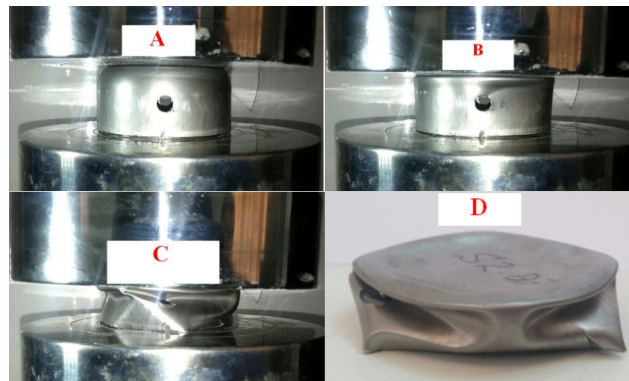


Fig. 12. Crushing process of S2-2C-D7 sample at a) Start of crushing process, b) Start of buckling, c) At the end of crushing step; d) The completely crushed S2-4C-D5 sample.

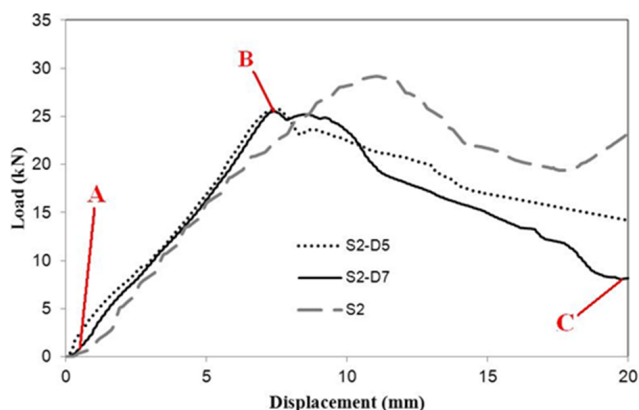


Fig. 13. Comparison of load-displacement curves for S2 (without trigger), S2-4C-D5 (with 4 cutouts of 5mm diameter) and S2-2C-D7 (with 2 cutouts of 7mm diameter).

This result may be attributed to symmetrical placement and the number of cutouts (4 symmetrical cutouts compared to two) in S2-4C-D5 sample. The undesired effects of triggers in reducing the absorbed energy was reported by some researchers like Daneshi and Hosseini-pour [34]. In contrast, other researchers like Samer et al. [18] showed that by increasing the number of cutouts and decreasing their diameter, the induced folds turned more stable and regular, and the initial peak force decreased, whereas the absorbed energy was improved. Cheng et al. [35] could also decrease the maximum load and increase the absorbed energy simultaneously in their AA6061-T6 aluminum square tubes inserting slotted and elliptical disconti-

nities. They showed that the triggered samples could change the deformation mode from global bending to splitting and cutting.

In the study by Han et al. [21], the results indicated that in quasi-static crushing test, if the location of cutout triggers moves from center of the sample toward the upper end of the tube, energy absorption capacity improves and crushing mode changes from axial crushing (concertina) to progressive buckling (diamond). Figs. 12 and 13 show that during the elastic crushing region (region A-B) of S2-2C-D7 sample, the crushing mode can be considered as an axial crushing. As the crushing force increases, the induced stress around the region with cutouts exceeds the yield limit and the sample yields earlier than S2 sample (region B). In this point and as the material initially yields (point B), the crushing mode changes to progressive buckling mode (region B-C). The S2-4C-D5 sample crushing mode and behavior is exactly similar to S2-2C-D7 sample, except that the plastic phase in triggered region for the S2-2C-D7 due to the bigger effective cross-section area begins a bit later. Moreover, in S2-4C-D5 sample due to the more symmetrical insertion of four circular cutouts, a more regular deformation was observed.

In addition to Han et al. [21], Samer et al.[18] also showed that creating cutout triggers lead to decrease in peak crushing force as well as increase in energy absorption if cutouts are placed at ideal locations, and their size and number are appropriately adopted. By comparing the crushing behavior of the S2-2C-D7 and S2-4C-D5 samples in the plastic crushing phase, it can be observed that by increasing the number and decreasing the diameter of cutouts, progressive folding occurs more regularly in the S2-4C-D5. This in turn, causes more steady force level (in the force-displacement curve) and finally higher energy absorption capacity in this sample.

Different energy absorption parameters of S2, S2-2C-D7 and S2-4C-D5 samples are compared in Figs. 14 and 15. As shown in Fig. 14, the specific absorbed energy (SAE) of S2-2C-D7 and S2-4C-D5 samples decreased compared with intact sample (S2) by about 12% and 3%, respectively. Although the number and diameter of cutouts did not affect significantly the initial peak force and the crushing distance at maximum force, they could improve the energy absorption in the sample with more circular cutouts with smaller diameter (S2-4C-D5) by about 10.6% relative to S2-2C-D7. As discussed, geometrical triggers can usually enhance the regularity and stability of samples deformation and generally reduce the induced stresses in the samples (see Fig. 15). Therefore, the vulnerable effects of impact on other parts of the structure (e.g. the passengers' cabin in automobiles) may be reduced [10]. This shows clearly the great importance of geometrical triggers.

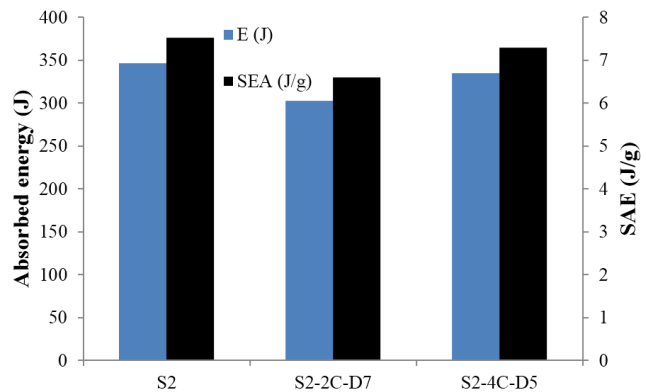


Fig. 14. Comparison of energy absorption and specific absorbed energy (SAE) of S2, S2-2C-D7 and S2-4C-D5 samples.

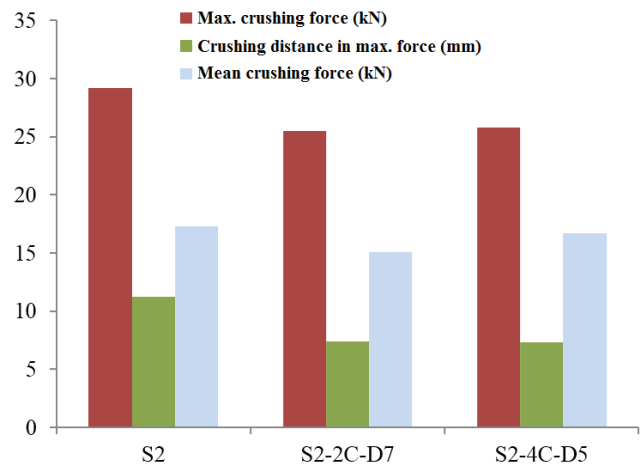


Fig. 15. Comparison between energy absorption parameters including maximum crushing force, crushing length at maximum force and average crushing force of S2, S2-2C-D7 and S2-4C-D5 samples.

5. Conclusions

Based on the results presented in this article, the following conclusions may be drawn:

- Increasing the thickness of core polymer layer from 1 to 2mm led to increase of initial maximum crushing force and the absorbed energy by about 16% and 24%, respectively.
- Crushing length in the first maximum crushing force increases by near 12% after increasing the thickness of polymer layer from 1 to 2mm.
- Circular cutout triggers with radii of 2.5 and 3.5mm result in 3.2% and 14.3% decrease in the amount of absorbed energy, respectively, compared to the intact samples.
- Despite lower energy absorption in triggered samples, lower first peak forces were also observed in these samples. Therefore, less damage in the

triggered absorbing elements and in their possible attached structures may be expected.

References

- [1] F. İnce, H.S. Türkmen, Z. Mecitoğlu, N. Uludağ, I. Durgun, E. Altinok, H. Örenel, A numerical and experimental study on the impact behavior of box structures, *Procedia Eng.*, 10 (2011) 1736-1741.
- [2] G.C. Jacob, J.F. Fellers, S. Simunovic, J.M. Starbuck, Energy absorption in polymer composites for automotive crashworthiness, *J. Compos. Mater.*, 36(7) (2002) 813-850.
- [3] Y. Ma, T. Sugahara, Y. Yang, H. Hamada, A study on the energy absorption properties of carbon/aramid fiber filament winding composite tube, *Compos. Struct.*, 123 (2015) 301-311.
- [4] M. Weiss, M.E. Dingle, B.F. Rolfe, P.D. Hodgson, The influence of temperature on the forming behavior of metal/polymer laminates in sheet metal forming, *ASME J. Eng. Mater. Technol.*, 129(4) (2007) 530-537.
- [5] A. Alavi Nia, H. Badnava, K. Fallah Nejad, An experimental investigation on crack effect on the mechanical behavior and energy absorption of thin-walled tubes, *Mater. Des.*, 32(6) (2011) 3594-3607.
- [6] A. Atrian, H. Panahi, Experimental and finite element investigation on wrinkling behaviour in deep drawing process of Al3105/Polypropylene/Steel304 sandwich sheets, *Procedia Manuf.*, 15 (2018) 984-991.
- [7] M.J. Jakirahemed, M.J. Davidson, G. Venkateswarlu, L. Venugopal, A study on effect of process parameters on the expansion of thin-walled aluminium 7075 tubes, *Int. J. Adv. Sci. Technol.*, 36 (2011) 83-94.
- [8] W.M. Choi, T.S. Kwon, H.S. Jung, J.S. Kim, Influence of impact velocity on energy absorption characteristics and friction coefficient of expansion tube, *Int. J. Crashworthiness*, 17(6) (2012) 1-9.
- [9] A. Alavi Nia, A. Akhavan Attar, The effect of different layouts in internal and external stiffeners on the energy absorption of thin-walled structures with square sections, *Arch. Civ. Mech. Eng.*, 17(4) (2017) 997-1010.
- [10] A. Praveen Kumar, M. Nalla Mohamed, A. Jusuf, T. Dirgantara, L. Gunawan, Axial crash performance of press-formed open and end-capped cylindrical tubes - A comparative analysis, *Thin-Walled Struct.*, 124 (2018) 468-488.
- [11] S.A. Galehdari, A.H. Hashemian, J.E. Jam, A. Atrian, A new approach to buckling analysis of lattice composite structures, *J. Solid Mech.*, 9(3) (2017) 599-607.
- [12] B.J. Ramirez, U. Misra, V. Gupta, Viscoelastic foam-filled lattice for high energy absorption, *Mech. Mater.*, 127 (2018) 39-47.
- [13] A. Alavi Nia, H. Khodabakhsh, The effect of radial distance of concentric thin-walled tubes on their energy absorption capability under axial dynamic and quasi-static loading, *Thin-Walled Struct.*, 93 (2015) 188-197.
- [14] F. Fereshteh-Saniee, A. Alavi Nia, A. Atrian, An experimental investigation on the deep drawing process of steel-brass bimetal sheets, 12th Int'l Conference Metal Forming, (2008) 63-70.
- [15] M. Parsa, Experimental and numerical determination of limiting drawing ratio of Al3105-Polypropylene-Al3105 sandwich sheets, *ASME J. Eng. Mater. Technol.*, 132(3) (2010) 031004.
- [16] S. Bagherzadeh, B. Mollaei-Darmani, K. Malekzadeh, Theoretical study on hydro-mechanical deep drawing process of bimetallic sheets and experimental observations, *J. Mater. Process. Technol.*, 212(9) (2012) 1840-1849.
- [17] H. Tsukamoto, Impact compressive behavior of deep-drawn cups consisting of aluminum/duralumin multi-layered graded structures, *Mater. Sci. Eng., A*, 198 (2015) 25-34.
- [18] F. Samer, F. Tariochan, P. Khalili, H. Samaka, Enhancement of energy absorption of thin walled hexagonal tube by using trigger mechanisms, *Int. J. Res. Eng. Tech.*, 2(8) (2013) 109-116.
- [19] N.N. Hussain, S.P. Regalla, Y.V.D. Rao, Comparative study of trigger configuration for enhancement of crashworthiness of automobile crash box subjected to axial impact loading, *Procedia Eng.*, 173 (2017) 1390-1398.
- [20] H. Jiang, Y. Ren, B. Gao, J. Xiang, F.G. Yuan, Design of novel plug-type triggers for composite square tubes: enhancement of energy-absorption capacity and inducing failure mechanisms, *Int. J. Mech. Sci.*, 131-132 (2017) 113-136.
- [21] H. Han, F. Taheri, N. Pegg, Quasi-static and dynamic crushing behaviors of aluminum and steel tubes with a cutout, *Thin-Walled Struct.*, 45(3) (2007) 283-300.
- [22] K.J. Kim, D. Kim, S.H. Choi, K. Chung, K.S. Shin, F. Barlat, K.H. Oh, J.R. Youn, Formability of AA5182/polypropylene/AA5182 sandwich sheets, *J. Mater. Process. Technol.*, 139(1-3) (2003) 1-7.

- [23] A. AlaviNia, A. Shirazi Beheshtiha, Investigation the effect of strain rate on mechanical behavior of aluminum thin-walled sections, 21st Annual International Conference on Mechanical Engineering-ISME2013, 7-9 May (2013).
- [24] F. Tarlochan, F. Samer, A.M.S. Hamouda, S. Rameshd, K. Khalid, Design of thin wall structures for energy absorption applications: Enhancement of crashworthiness due to axial and oblique impact forces, *Thin-Walled Struct.*, 71 (2013) 7-17.
- [25] Standard, Annual Book of ASTM Standards, 1st Edition, American Society for Testing Materials International, (2001).
- [26] A. Rajabi, M. Kadkhodayan, An experimental and numerical investigation of wrinkling in deep drawing of fiber-metal laminates, in 10th International Conference on Technology of Plasticity, ICTP 2011, Aachen, Sheet Metal Forming, (2011) 438-443.
- [27] A. Rajabi, M. Kadkhodayan, M. Manoochehri, R. Farjadfar, Deep-drawing of thermoplastic metal-composite structures: Experimental investigations, statistical analyses and finite element modeling, *J. Mater. Process. Technol.*, 215 (2015) 159-170.
- [28] H. Takuda, H. Fujimoto, N. Hatta, Formabilities of steel/aluminium alloy laminated composite sheets, *J. Mater. Sci.*, 33(1) (1998) 91-97.
- [29] J.U. Cho, S.J. Hong, S.K. Lee, C.D. Cho, Impact fracture behavior at the material of aluminum foam, *Mater. Sci. Eng. A*, 539 (2012) 250-258.
- [30] R. Kalhor, S.W. Case, The effect of FRP thickness on energy absorption of metal-FRP square tubes subjected to axial compressive loading, *Compos. Struct.*, 130 (2015) 44-50.
- [31] M.D. Goel, Deformation, energy absorption and crushing behavior of single-, double- and multi-wall foam filled square and circular tubes, *Thin-Walled Struct.*, 90 (2015) 1-11.
- [32] N. Peixinho, D. Soares, C. Vilarinho, P. Pereira, D. Dimas, Experimental study of impact energy absorption in aluminium square tubes with thermal triggers, *Mater. Res.*, 15(2) (2012) 323-332.
- [33] L. Abah, A. Limam, M. Dejeammes, Effects of cutouts on static and dynamic behaviour of square aluminium extrusions, *WIT Trans. Built Environ.*, 35 (1998) 10.
- [34] G.H. Daneshi, S.J. Hosseinipour, Grooves effect on crashworthiness characteristics of thin-walled tubes under axial compression. *Mate. Des.*, 23(7) (2002) 611-617.
- [35] Q. Cheng, W. Altenhof, L. Li, Experimental investigations on the crush behaviour of AA6061-T6 aluminum square tubes with different types of through-hole discontinuities, *Thin-Walled Struct.*, 44(4) (2006) 441-454.